J|A|C|S ARTICLES

Published on Web 11/24/2010

Structure−Function Analysis of an Enzymatic Prenyl Transfer Reaction Identifies a Reaction Chamber with Modifiable Specificity

Marco Jost,[†,‡] Georg Zocher,[†] Sylwia Tarcz,[§] Marco Matuschek,[§] Xiulan Xie,[||] Shu-Ming Li,[*,§] and Thilo Stehle[*,†,⊥]

Interfakultäres Institut für Biochemie, Universität Tübingen, Hoppe-Seyler-Strasse 4, 72076 Tübingen, Germany, Institut für Pharmazeutische Biologie und Biotechnologie, Universität Marburg, Deutschhausstrasse 17a, 35037 Marburg, Germany, Fachbereich Chemie, Universität Marburg, Hans-Meerwein-Strasse, 35032 Marburg, Germany, and Department of Pediatrics, Vanderbilt University School of Medicine, Nashville, Tennessee 37232, United States

Received July 30, 2010; E-mail: thilo.stehle@uni-tuebingen.de; shuming.li@staff.uni-marburg.de

Abstract: Fungal indole prenyltransferases participate in a multitude of biosynthetic pathways. Their ability to prenylate diverse substrates has attracted interest for potential use in chemoenzymatic synthesis. The fungal indole prenyltransferase FtmPT1 catalyzes the prenylation of brevianamide F in the biosynthesis of fumitremorgin-type alkaloids, which show diverse pharmacological activities and are promising candidates for the development of antitumor agents. Here, we report crystal structures of unliganded *Aspergillus fumigatus* FtmPT1 as well as of a ternary complex of FtmPT1 bound to brevianamide F and an analogue of its isoprenoid substrate dimethylallyl diphosphate. FtmPT1 assumes a rare α/β-barrel fold, consisting of 10 circularly arranged β-strands surrounded by α-helices. Catalysis is performed in a hydrophobic reaction chamber at the center of the barrel. In combination with mutagenesis experiments, our analysis of the liganded and unliganded structures provides insight into the mechanism of catalysis and the determinants of regiospecificity. Sequence conservation of key features indicates that all fungal indole prenyltransferases possess similar active site architectures. However, while the dimethylallyl diphosphate binding site is strictly conserved in these enzymes, subtle changes in the reaction chamber likely allow for the accommodation of diverse aromatic substrates for prenylation. In support of this concept, we were able to redirect the regioselectivity of FtmPT1 by a single mutation of glycine 115 to threonine. This finding provides support for a potential use of fungal indole prenyltransferases as modifiable bioreactors that can be engineered to catalyze highly specific prenyl transfer reactions.

Introduction

The transfer of prenyl moieties is a common reaction in metabolic processes. Such transfers occur, for example, during the attachment of prenyl anchors to cysteine residues by the action of protein prenyltransferases (PTs), during terpenoid biosynthesis, catalyzed by *trans*-PTs, and during the biosynthesis of some prenylated aromatic compounds including the primary metabolites ubiquinone and menaquinone as well as several plant secondary metabolites, performed by the group of membrane-bound "aromatic" PTs.[1−7] All of these enzymes contain one or more conserved (N/D)DXXD motifs that are essential for prenyl diphosphate binding via divalent cations. Consequently, these enzymes also depend on the presence of Mg^{2+} or Mn^{2+}.[3] In addition, a number of soluble aromatic PTs were identified in bacteria and fungi. This group of PTs can be further subdivided into three clusters, depending on sequence similarity. Members of the first cluster, termed "ABBA-PTs" due to the occurrence of several $\alpha\beta\beta\alpha$-repeats in their structure, are primarily of bacterial origin. Three new members of this cluster were reported very recently from ascomycetous fungi.[8] These proteins share no similarities with the previously described classes of PTs, although a few of them are dependent on divalent cations.[9] The members of the second cluster are indole prenyltransferases from different bacteria.[10] The third cluster mainly consists of

[†] Universität Tübingen.
[‡] Current address: Department of Chemistry, Massachusetts Institute of Technology, Cambridge, MA 02139.
[§] Institut für Pharmazeutische Biologie und Biotechnologie, Universität Marburg.
[||] Fachbereich Chemie, Universität Marburg.
[⊥] Vanderbilt University School of Medicine.

(1) Sacchettini, J. C.; Poulter, C. D. *Science* **1997**, *277*, 1788.
(2) Bohlmann, J.; Meyer-Gauen, G.; Croteau, R. *Proc. Natl. Acad. Sci. U.S.A.* **1998**, *95*, 4126.
(3) Liang, P. H.; Ko, T. P.; Wang, A. H. *Eur. J. Biochem.* **2002**, *269*, 3339.
(4) Ashby, M. N.; Kutsunai, S. Y.; Ackerman, S.; Tzagoloff, A.; Edwards, P. A. *J. Biol. Chem.* **1992**, *267*, 4128.
(5) Suvarna, K.; Stevenson, D.; Meganathan, R.; Hudspeth, M. E. *J. Bacteriol.* **1998**, *180*, 2782.
(6) Turunen, M.; Olsson, J.; Dallner, G. *Biochim. Biophys. Acta* **2004**, *1660*, 171.
(7) Yazaki, K.; Sasaki, K.; Tsurumaru, Y. *Phytochemistry* **2009**, *70*, 1739.
(8) Haug-Schifferdecker, E.; Arican, D.; Brueckner, R.; Heide, L. *J. Biol. Chem.* **2010**, *285*, 16487.
(9) Tello, M.; Kuzuyama, T.; Heide, L.; Noel, J. P.; Richard, S. B. *Cell. Mol. Life Sci.* **2008**, *65*, 1459.
(10) Takahashi, S.; Takagi, H.; Toyoda, A.; Uramoto, N.; Nogawa, T.; Ueki, M.; Sakaki, Y.; Osada, H. *J. Bacteriol.* **2010**, *192*, 2839.

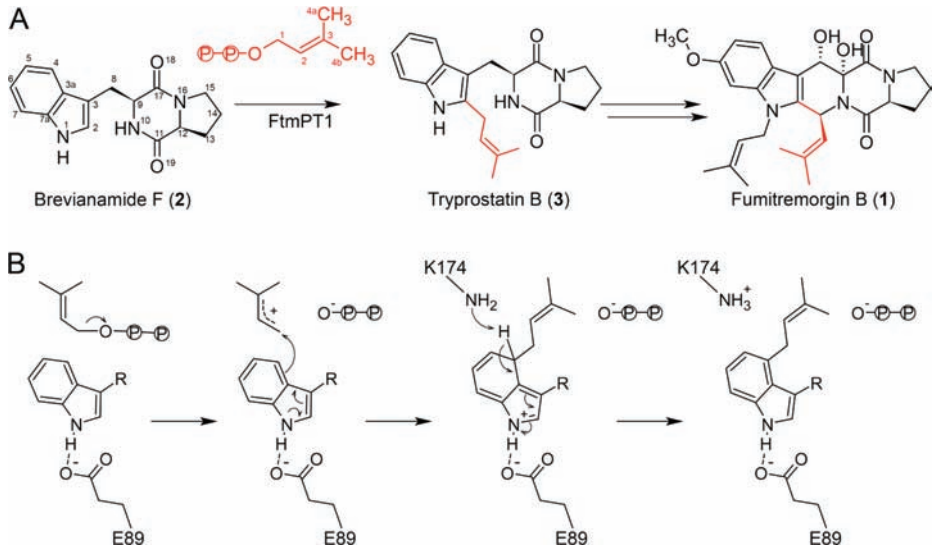

Figure 1. Reactions catalyzed by FtmPT1 and FgaPT2. (A) Reaction catalyzed by FtmPT1. Numberings of brevianamide F (**1**) and dimethylallyl diphosphate (red) are indicated as used throughout this work. (B) Putative reaction mechanism of FgaPT2.[32] In this case, the aromatic substrate is L-Trp.

fungal indole PTs, many of which were biochemically characterized over the last years.[11,12] These enzymes exhibit very little sequence similarities with all other classes of PTs, they do not possess a (N/D)DXXD motif, and their catalytic activities do not depend on the presence of divalent cations.[11]

The fungal indole PTs are involved as key enzymes in the biosynthetic pathways of several fungal indole alkaloids and catalyze the prenylation of tryptophan or its derivatives.[12,13] Prominent examples of prenylated indole alkaloids include the terrequinone alkaloids, such as terrequinone A,[14] and the ergot alkaloids, such as fumigaclavine C from *Aspergillus fumigatus* or ergotamine from the parasitic fungus *Claviceps purpurea*. Ergotamine was found to be responsible for "ergotism" and "antonius fire" during the middle ages, and derivatives are used as drugs in modern medicine.[15] The fungal indole PTs show varying substrate specificities and exhibit different regiospecificities in attaching the prenyl group to carbon or nitrogen atoms of the indole nucleus. In principle, prenylation can occur in two different ways: A "regular" prenylation attaches the prenyl group via its C-1 atom (Figure 1A) to the substrate, whereas a "reverse" prenylation links the C-3 atom with the substrate. Fungal indole PTs can carry out both types of prenylation, and they exhibit remarkable flexibility for their aromatic substrates.[11,12] The prenylation products and derivatives thereof exhibit multiple pharmacological activities. Thus, this group of enzymes is of considerable interest for the chemoenzymatic synthesis of bioactive compounds.[11,12,16,17]

Fumitremorgin B (**1** in Figure 1A), a mycotoxin with tremorgenic activity, is produced by various fungi of the genera *Aspergillus* and *Penicillium*. Its biosynthetic intermediates such as tryprostatin A and B as well as fumitremorgin C exhibit diverse biological activities of pharmaceutical and medicinal interest. Fumitremorgin C is a potent and specific chemosensitizing agent and reverts multidrug resistance in cells transfected with the breast cancer resistance protein (BCRP).[18,19] Tryprostatin A is also able to inhibit the ABC transporter BCRP.[20,21] Furthermore, both tryprostatin B and A exhibit high cytotoxicity toward various cancer cell lines with a higher potency than etoposide.[22] Therefore, tryprostatin A, tryprostatin B, and fumitremorgin C as well as their derivatives are promising candidates for the development of anticancer agents. Compounds closely related to fumitremorgin C have already been shown to inhibit BCRP at similar levels but with reduced cytotoxicity.[23,24]

Fumitremorgin B was first isolated from *A. fumigatus* in 1971.[25] Its chemical structure features a modified cyclic dipeptide of L-tryptophan (L-Trp) and L-proline (L-Pro).[26] Chemical modifications include two prenylations at C-2 and N-1 of the indole nucleus of L-Trp. Hence, the biosynthesis of fumitremorgin B was predicted to include a prenylation step of *cyclo*-L-Trp-L-Pro (Brevianamide F, **2**) at C-2 of the indole nucleus to yield tryprostatin B (**3**, Figure 1A).[13,27] Two prenyltransferase genes, termed *ftmPT1* and *ftmPT2*, were identified in the biosynthetic gene cluster of fumitremorgin-

(11) Steffan, N.; Grundmann, A.; Yin, W.-B.; Kremer, A.; Li, S.-M. *Curr. Med. Chem.* **2009**, *16*, 218.
(12) Li, S.-M. *Nat. Prod. Rep.* **2010**, *27*, 57.
(13) Williams, R. M.; Stocking, E. M.; Sanz-Cervera, J. F. In *Biosynthesis: Aromatic Polyketides, Isoprenoids, Alkaloids*; Leeper, F. J., Vederas, J. C., Eds.; Springer-Verlag: Berlin Heidelberg, 2000; Vol. 209, p 98.
(14) Balibar, C. J.; Howard-Jones, A. R.; Walsh, C. T. *Nat. Chem. Biol.* **2007**, *3*, 584.
(15) Haarmann, T.; Rolke, Y.; Giesbert, S.; Tudzynski, P. *Mol. Plant. Pathol.* **2009**, *10*, 563.
(16) Li, S. M. *Appl. Microbiol. Biotechnol.* **2009**, *84*, 631.
(17) Li, S.-M. *Phytochemistry* **2009**, *70*, 1746.
(18) Rabindran, S. K.; He, H.; Singh, M.; Brown, E.; Collins, K.; Annable, T.; Greenberger, L. M. *Cancer Res.* **1998**, *58*, 5850.
(19) Rabindran, S. K.; Ross, D. D.; Doyle, L. A.; Yang, W.; Greenberger, L. M. *Cancer Res.* **2000**, *60*, 47.
(20) Woehlecke, H.; Osada, H.; Herrmann, A.; Lage, H. *Int. J. Cancer* **2003**, *107*, 721.
(21) Jain, H. D.; Zhang, C.; Zhou, S.; Zhou, H.; Ma, J.; Liu, X.; Liao, X.; Deveau, A. M.; Dieckhaus, C. M.; Johnson, M. A.; Smith, K. S.; Macdonald, T. L.; Kakeya, H.; Osada, H.; Cook, J. M. *Bioorg. Med. Chem.* **2008**, *16*, 4626.
(22) Zhao, S.; Smith, K. S.; Deveau, A. M.; Dieckhaus, C. M.; Johnson, M. A.; Macdonald, T. L.; Cook, J. M. *J. Med. Chem.* **2002**, *45*, 1559.
(23) van Loevezijn, A.; Allen, J. D.; Schinkel, A. H.; Koomen, G.-J. *Bioorg. Med. Chem. Lett.* **2001**, *11*, 29.
(24) Allen, J. D.; van Loevezijn, A.; Lakhal, J. M.; van der Valk, M.; van Tellingen, O.; Reid, G.; Schellens, J. H. M.; Koomen, G.-J.; Schinkel, A. H. *Mol. Cancer Ther.* **2002**, *1*, 417.
(25) Yamazaki, M.; Suzuki, S.; Miyaki, K. *Chem. Pharm. Bull.* **1971**, *19*, 1739.
(26) Yamazaki, M.; Sasago, K.; Miyaki, K. *J. Chem. Soc., Chem. Commun.* **1974**, *40*, 408.
(27) Cui, C. B.; Kakeya, H.; Osada, H. *J. Antibiot.* **1996**, *49*, 534.

type alkaloids by mining of the *A. fumigatus* genome.[28,29] The postulated brevianamide F prenyltransferase FtmPT1 was purified and characterized after heterologous expression in *E. coli*.[28] Biochemical data showed that brevianamide F was prenylated regularly by FtmPT1 at C-2, resulting in formation of tryprostatin B. By using tryptophan and derivatives as substrates, N-1 reversely prenylated products were obtained in the incubation mixtures with FtmPT1.[30] Interestingly, reverse prenylation of brevianamide F is also observed at position C-2 in different pathways leading to the formation of the brevianamides, the austamides, and the paraherquamides.[13,31]

The first structure of a soluble fungal indole PT, 4-dimethylallyl tryptophan synthase (4-DMATS, FgaPT2) from *A. fumigatus*, revealed that the enzyme possesses a rare α/β barrel fold termed the prenyltransferase barrel (PT barrel).[32] FgaPT2 catalyzes the first committed step in ergot alkaloid biosynthesis, a regular prenylation of L-Trp at position C-4 of the indole nucleus.[33] On the basis of the crystal structure, a three-step reaction mechanism was proposed that involves formation of a dimethylallylic cation, subsequent nucleophilic attack of this cation by the indole nucleus to form the σ-complex, and deprotonation to release the final product (Figure 1B).[32] The PT barrel is also present in the crystal structures of the bacterial aromatic PTs NphB, formerly named Orf2, and CloQ.[34,35] NphB and CloQ are involved in the biosynthetic pathways of the antioxidant naphterpin and the antibiotic clorobiocin, respectively.[34,36] Both enzymes belong to the group of ABBA-PTs and exhibit no sequence similarity to FgaPT2 and FtmPT1. Nevertheless, on the basis of the uniqueness of the fold, it was proposed that these PTs share a common evolutionary origin.[32] NphB catalyzes a regular C-prenylation of various aromatic substrates such as 1,6-dihydroxynaphthalene using geranyl diphosphate as the prenyl donor.[34] The natural aromatic substrate of NphB is unknown. CloQ was shown to prenylate 4-hydroxyphenylpyruvate using DMAPP to yield 3-dimethylallyl-4-hydroxyphenylpyruvate.[36]

Here, we report the crystallization and X-ray structural analysis of FtmPT1, a soluble aromatic PT catalyzing the second step in the biosynthesis of fumitremorgin-type alkaloids in *A. fumigatus*. Like FgaPT2, the structure of FtmPT1 belongs to the PT barrel family. Nevertheless, both enzymes accept different substrates and perform catalysis with different regiospecificity. Structural analysis of FtmPT1 in complex with substrates and a substrate analogue provides insight into the mechanisms of catalysis and the determinants of regiospecificity in soluble aromatic PTs. Furthermore, we were able to modify the enzymatic activity of FtmPT1 to perform a reverse prenylation at the atom C-3 of the indole nucleus by a single point mutation.

Results

Overall Structure of FtmPT1. The crystal structure of unliganded FtmPT1 was determined at 2.50 Å resolution by molecular replacement using a modified crystal structure of FgaPT2.[32] We then produced a ternary complex of FtmPT1 by soaking crystals with the substrate brevianamide F and a nonhydrolyzable analogue of dimethylallyl diphosphate (DMAPP), dimethylallyl *S*-thiolodiphosphate (DMSPP), and determined its structure at 2.40 Å resolution. Data collection and refinement statistics for both structures are given in the Supporting Information (Tables S2 and S3).

The overall three-dimensional structure of FtmPT1 is formed by a central core of 10 antiparallel β-strands that are surrounded by a ring of 10 partially solvent-exposed α-helices (Figure 2A). The secondary structure elements are arranged in five structurally similar $\alpha\alpha\beta\beta$ repeats. In each of these repeats, the two α-helices pack tightly against the two β-strand units, stabilizing the overall structure with hydrophobic contacts. The 10 β-strands form a large solvent-filled barrel, in which the substrates are bound and catalysis is performed. FtmPT1 exists as a dimer in solution and also forms dimers in the crystal (Supporting Information, Figure S1A−C). The crystallographic dimer is highly similar to a dimer observed in the FgaPT2 structure,[32] despite different crystal packing environments. The physiologic relevance of dimer formation is unclear in both cases, as amino acids involved in interface formation do not participate in binding of ligands in either FgaPT2 or FtmPT1.

A search for structural homologues using DaliLite[37] yielded only two proteins, FgaPT2 and NphB, which possess significant similarity to FtmPT1 (*Z*-scores of 54.8 and 16.5, respectively). On the basis of these analyses, FtmPT1 is a member of the PT barrel family, which presently only includes FgaPT2, NphB, and CloQ. The coordinates of CloQ were not available at the time of writing of this article. With 464 residues, FtmPT1 is very similar in size to FgaPT2 (459 residues) and significantly larger than NphB (307 residues), although all three share the same domain structure. In FgaPT2 and FtmPT1, the additional residues are found in extended loop regions. The superposition with FgaPT2 (Figure 2A) is excellent (C_α-rmsd 1.3 Å for 402 aligned residues), whereas there are some structural differences between FtmPT1 and NphB (C_α-rmsd 3.6 Å for 301 aligned residues). Although the core structures of the bacterial naphthalene PT NphB and the fungal indole PT FtmPT1 agree well with each other, the active sites of these two PTs differ substantially. On the other hand, the active site architectures of FgaPT2 and FtmPT1 are more conserved. Therefore, structural comparisons are only carried out using the structures of FtmPT1 and FgaPT2. We expect that conclusions from these analyses can then be applied to other, structurally unknown but homologous, fungal indole PTs.

The Active Site of FtmPT1. The substrate-bound structure of FtmPT1 revealed the binding mode for its substrates (Figure 2A−C). Brevianamide F binds near the center of the PT barrel (Figure 2A,C). Given the aromatic character of the substrate, it is not surprising that interactions with FtmPT1 involve many hydrophobic residues (Y435, Y203, L96, L187, M94, M364,

(28) Grundmann, A.; Li, S.-M. *Microbiology* **2005**, *151*, 2199.
(29) Grundmann, A.; Kuznetsova, T.; Afiyatullov, S. S.; Li, S. M. *ChemBioChem* **2008**, *9*, 2059.
(30) Zou, H.; Zheng, X.; Li, S.-M. *J. Nat. Prod.* **2009**, *72*, 44.
(31) Ding, Y.; de Wet, J. R.; Cavalcoli, J.; Li, S.; Greshock, T. J.; Miller, K. A.; Finefield, J. M.; Sunderhaus, J. D.; McAfoos, T. J.; Tsukamoto, S.; Williams, R. M.; Sherman, D. H. *J. Am. Chem. Soc.* **2010**, *132*, 12733.
(32) Metzger, U.; Schall, C.; Zocher, G.; Unsöld, I. A.; Stec, E.; Li, S.-M.; Heide, L.; Stehle, T. *Proc. Natl. Acad. Sci. U.S.A.* **2009**, *106*, 14309.
(33) Unsöld, I. A.; Li, S.-M. *Microbiology* **2005**, *151*, 1499.
(34) Kuzuyama, T.; Noel, J. P.; Richard, S. B. *Nature* **2005**, *435*, 983.
(35) Metzger, U.; Keller, S.; Stevenson, C. E.; Heide, L.; Lawson, D. M. *J. Mol. Biol.* **2010**, in press.
(36) Pojer, F.; Wemakor, E.; Kammerer, B.; Chen, H.; Walsh, C. T.; Li, S. M.; Heide, L. *Proc. Natl. Acad. Sci. U.S.A.* **2003**, *100*, 2316.
(37) Holm, L.; Kaariainen, S.; Rosenstrom, P.; Schenkel, A. *Bioinformatics* **2008**, *24*, 2780.

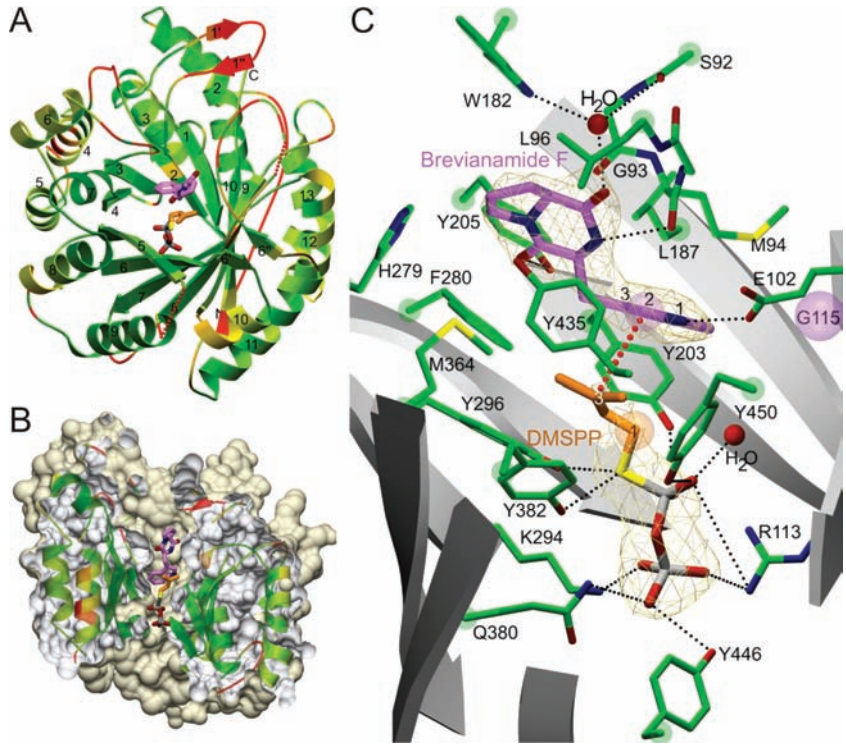

Figure 2. Structure of FtmPT1. (A) Overall fold of the substrate-bound FtmPT1 in cartoon representation. C_α-atoms of FtmPT1 are colored by rmsd difference to positions of C_α-atoms in the crystal structure of FgaPT2 from green (zero rmsd difference) to red (rmsd difference above 3 Å). The substrates brevianamide F (violet) and DMSPP (orange) are depicted in stick representation. Red dashed lines indicate a gap in the structure as a result of disordered amino acids. (B) Cross section of the PT barrel of FtmPT1 depicting the positions of DMSPP (orange) and brevianamide F (violet) in the central reaction cavity. (C) Cross section of the active site of FtmPT1 with the bound substrates. A ($2F_{obs} - F_{calc}$) simulated annealing omit map (yellow mesh) is shown around brevianamide F (violet) at a contour level of 1.5 σ and around DMSPP (orange) at a contour level of 1.0 σ. Reacting atoms of DMSPP and brevianamide F are emphasized with transparent spheres. Furthermore, atoms C-1 and C-3 of DMSPP and atoms N-1, C-2, and C-3 of brevianamide F are labeled. Hydrogen bonds and ionic interactions are depicted by dotted black lines. The closest atom to the location of prenylation, C-2 of the indole nucleus, is the atom C-3 of the DMSPP, as shown by the dotted red line. G115 is indicated as a violet sphere.

and F280) that line a large pocket (Figure 2C and Supporting Information, Figure S2). In addition, brevianamide F is also held in place via a network of hydrogen bonds in which all of its polar groups participate. The indole nitrogen N-1 is linked by a hydrogen bond to the carboxylate group of E102, which is conserved in all fungal indole PTs. O-18 of the diketopiperazine moiety forms a direct hydrogen bond to the Y205 hydroxyl group. O-19 is linked, via a water molecule, to the backbone carbonyl of S92 and the W182 side chain nitrogen. Finally, N-10 is hydrogen bonded to the backbone carbonyl of M94, albeit with less than ideal geometry (Figure 2C).

The substrate analogue DMSPP binds near the upper and central parts of the barrel. Strong electron density is observed for the pyrophosphate moiety of DMSPP, whereas the electron density for the dimethylallyl group is somewhat weaker (Figure 2C), perhaps as a result of some mobility or competitive binding of sulfate ions from the crystallization buffer. As the binding site for DMAPP is conserved for FgaPT2 and FtmPT1, we used the substrate-bound structure of FgaPT2 in addition to the electron density for modeling of the dimethylallyl group of DMSPP.

Contacts to DMSPP are contributed by residues located in the N-terminal and central regions of strands 2, 4, 6, 8, and 10. Two positively charged residues, R113 and K294, anchor the terminal phosphate group (Figure 2C and Supporting Information, Figure S2). In addition, the side chains of Q380 and Y446 contribute hydrogen bonds to the terminal phosphate. The bridging phosphate is bound via a salt bridge to R113 and hydrogen bonds to the hydroxyl groups of Y203 and Y450. A cluster of five aromatic residues (Y203, Y296, F280, Y382, and Y450) lies at the center of the barrel. The side chains of these residues are partially solvent-exposed. The hydroxyl groups of four tyrosine residues form a ring-shaped "tyrosine shield" that separates a more occluded hydrophobic pocket in the lower part of the barrel, which binds brevianamide F and the dimethylallyl moiety, from the solvent-accessible diphosphate binding site at the top of the barrel. Upon binding of DMSPP, the dimethylallyl part is inserted into the hydrophobic pocket, while the bridging phosphate is bound by the hydroxyl groups. The tyrosine shield is likely essential for catalysis as it protects the nascent dimethylallylic cation, generated by cleavage of the phosphoric acid ester, from nucleophilic attack by water or other components of the solvent.

FtmPT1 does not undergo any major changes in the orientations of side chains upon substrate binding. The only significant difference between the native and the substrate-bound structure is a subtle conformational change of the loop comprising residues 336−363, which also results in lower thermal mobility of this region (Supporting Information, Figure S3). In addition, a conformational change for Y446 is observed, although the electron density suggests that this residue is relatively flexible in both the native and the substrate-bound state. This comparatively small change upon ligand engagement is in vast contrast to the situation in FgaPT2, where several side chains were found to undergo considerable movement upon L-Trp and DMSPP binding, leading to a dramatic rearrangement of the active site.[32] The majority of these changes occurred in the DMAPP binding site. The structural changes in FgaPT2 can be explained by the

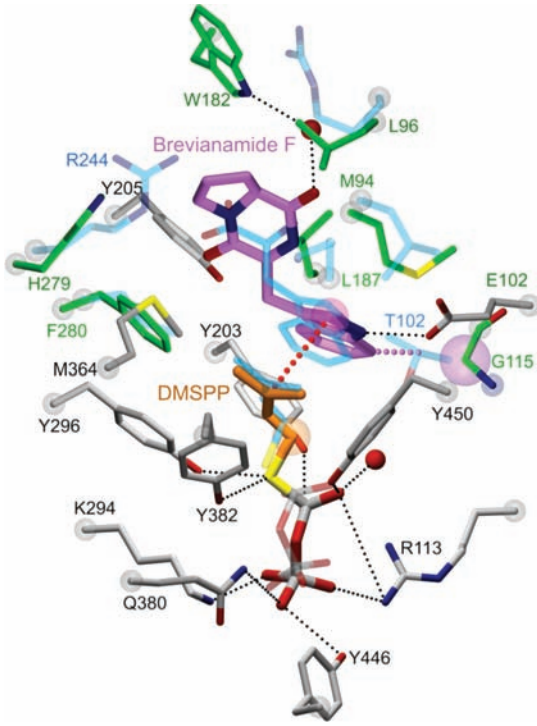

Figure 3. Comparison of substrate binding in FtmPT1 and FgaPT2. Amino acids that are equivalent in FtmPT1 and FgaPT2 are shown in gray. Carbon atoms of residues that differ between FtmPT1 and FgaPT2 are shown in green and transparent blue, respectively. The binding site of FtmPT1 is substantially enlarged by the replacement of T102 in FgaPT2 with G115 (violet sphere), which causes brevianamide F (violet) to slide further into the binding site as compared to the binding of L-Trp in FgaPT2 (blue, transparent). The carbon atoms of DMSPP are shown in orange and transparent blue for FtmPT1 and FgaPT2, respectively.

repulsive electrostatic forces among several basic residues in the absence of pyrophosphate. Once DMSPP binds, these side chains can swing into place to neutralize the negative charges of the phosphate groups. The active site of unliganded FtmPT1 contains a sulfate ion, which occupies the same space as the terminal phosphate of DMSPP in the substrate-bound structure (Supporting Information, Figure S3). This sulfate probably stabilizes the basic residues surrounding the active site and reduces electrostatic repulsion. Replacement of the sulfate with the pyrophosphate group is therefore not expected to lead to a dramatic change in overall electrostatic forces or in side chain conformations. The presence of sulfate in unliganded FtmPT1 probably accounts for the weaker binding of DMSPP compared to brevianamide F in our soaking experiments, as it suggests that sulfate and DMSPP would compete for binding. Also, it is likely that due to the presence of sulfate in the crystallization buffer, several side chains have already adopted their substrate-bound conformations in the native structure. This would lead to a reduction of flexibility at the active site, thus making it more difficult to incorporate DMSPP.

Comparison of the Active Sites of FtmPT1 and FgaPT2. The structures of FtmPT1 and FgaPT2,[32] including the organization of their catalytic centers, superimpose very well with each other (Figures 2A and 3). A structure-based sequence alignment of FtmPT1 and FgaPT2 demonstrates the high degree of conservation of catalytic residues (Supporting Information, Figure S4). Positions and binding modes of the DMAPP substrate analogue are virtually identical in both enzymes (Figure 3). Despite this conservation of one of the substrates, FtmPT1 and FgaPT2 clearly differ in their specificity for the second substrate, as well as in their regioselectivity. While FgaPT2 uses L-Trp as a substrate and transfers the prenyl group to atom C-4 of the indole nucleus, FtmPT1 uses the cyclic dipeptide brevianamide F as a substrate and transfers the prenyl group to atom C-2 of the indole nucleus. The structural basis for these differences is evident from the substrate-bound structures. Many side chains in the two pockets have similar characteristics and perform generally similar functions (Figure 3). However, the binding pocket of FtmPT1 is substantially enlarged as a result of substitutions at two key positions. FgaPT2 residue T102, which is located at the rear of the binding pocket, is replaced with G115 in FtmPT1. Furthermore, R244, which binds the carboxylate group of L-Trp in FgaPT2, is replaced with H279 (Figure 3). These two substitutions allow FtmPT1 to accommodate the larger substrate brevianamide F. They also account for differences in location of the two substrates (Figure 3). The position of the indole ring of brevianamide F is shifted by about 1 Å further into the binding pocket in comparison to that of L-Trp in FgaPT2. This shift can primarily be attributed to the substitution of G115 for T102 as the absence of a side chain in G115 allows the indole ring to slide deeper into the binding pocket. The indole ring of brevianamide F is also tilted away from the DMSPP by about 18° as compared to its position in FgaPT2 (Figure 3). This tilt is probably facilitated by the replacement of L81 in FgaPT2 with M94 in FtmPT1, as the unbranched methionine side chain allows the indole ring to approach more closely. The altered position of the indole ring in FtmPT1 places its C-4, C-5, C-6, and C-7 atoms far away from the dimethylallyl moiety. Thus, although FtmPT1 and FgaPT2 share a very similar overall fold and bind DMSPP in a similar fashion, differences in the binding sites lead to subtle repositioning of the second, aromatic substrate, accounting for the observed differences in the regioselectivities of these enzymes.

Structural Basis for the Reaction Mechanism of FtmPT1. FtmPT1 catalyzes an electrophilic alkylation, or Friedel−Crafts alkylation, that resembles the reaction catalyzed by FgaPT2, albeit with different regioselectivity. The proposed reaction mechanism of FgaPT2 contains three steps (Figure 1B) and is probably very similar to that of FtmPT1. The substrate-bound structure of FtmPT1 provides an excellent basis for investigating the catalytic mechanism of this reaction. The reaction is most likely initiated by hydrolysis of the phosphoric acid ester bond to form the dimethylallylic cation and a pyrophosphate group. This carbocation formation, which requires strong Lewis acids in chemical synthesis, is facilitated by interactions of the pyrophosphate group with the positively charged residues in the pyrophosphate binding site (Figure 2C). Evidence for a carbocation intermediate in the reaction of FgaPT2 was recently found by Luk and Tanner using positional isotope exchange and kinetic isotope effect experiments.[38] Given the overall similarity of the active sites of FgaPT2 and FtmPT1 and the nearly identical surroundings of DMSPP in both structures, we think it is likely that both enzymes use the same dissociative mechanism. The resulting carbocation, in which the positive charge is delocalized between the atoms C-1 and C-3, would be stabilized from two sides by cation−π interactions with aromatic ring systems, one from the substrate brevianamide F and one from the side chain of Y382 (Figure 2C). The stabilized cation can then undergo a nucleophilic attack from an aromatic nucleus such as that of the indole. The reactivity of the indole

(38) Luk, L. Y.; Tanner, M. E. *J. Am. Chem. Soc.* **2009**, *131*, 13932.

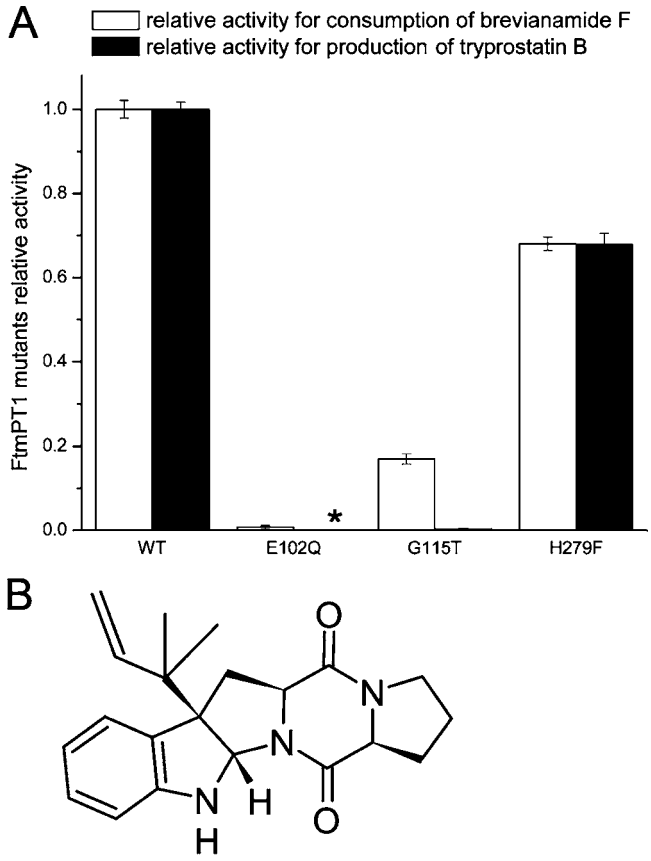

Figure 4. Mutagenesis experiments of FtmPT1. (A) Relative activity of the FtmPT1 E102Q, G115T, and H279F mutants for the consumption of brevianamide F and the production of tryprostatin B. Error bars denote deviation of two measurements. *No production of tryprostatin B could be detected for the E102Q mutant under assay conditions used in this study. (B) Chemical structure of the new product of the G115T mutant.

is likely enhanced by a hydrogen bond from its N-1 nitrogen to the side chain carboxylate of E102 (Figure 2C). Although position C-2 is already the most reactive site of a C-3-substituted indole, this hydrogen bond presumably contributes to the reactivity. Interaction of the carboxylate with the N-1 would further increase the nucleophilicity of the indole nucleus and stabilize the positive charge of the σ-complex, which is formed by the nucleophilic attack. An essential role of E102 in the catalytic cycle is supported by mutagenesis studies. The conservative mutation of E102 to Q reduced the production of tryprostatin B to undetectable amounts (Figure 4A). As Q102 can still form a hydrogen bond to the indole N-1, it appears that the negative charge of E102 is required for catalysis. In addition to increasing the reactivity of the indole, the E102 side chain could also help to deprotonate this complex to form the final product.

To investigate the identity of the base performing proton abstraction from the σ-complex, we performed additional site-directed mutagenesis. Two residues that could act as a base, E102 and H279, lie in the vicinity of the indole C-2 atom and must therefore be considered. As demonstrated by the analysis of the E102Q mutation, the E102 side chain is clearly critical for catalysis (Figure 4A). It is possible that E102 can act as a base. To test the influence of H279 on the catalytic cycle, we produced a H279F mutant that maintains aromatic properties of the side chain while eliminating its capacity to accept or donate protons. Histidine and phenylalanine also have similar-sized side chains, further reducing the risk of larger structural rearrangements triggered by the mutation. The H279F mutant protein has a relative activity of 70%, both for the consumption of brevianamide F and for the production of tryprostatin B (Figure 4A). This result strongly suggests that H279 does not participate in acid−base catalysis and indicates that proton abstraction at C-2 occurs either by E102 serving as a base or by the amide nitrogen of the diketopiperazine moiety.

We then examined the relative orientation of the substrates to gain insight into the mechanisms underlying the regioselectivity of FtmPT1. A dimethylallylic cation can react via its atoms C-1 or C-3, which would result in regular or reverse prenylations, respectively. Distances of 3.5−3.9 Å were reported between the atoms C-4 to C-7 of the indole nucleus and the C-1 atoms of DMSPP in FgaPT2.[32] Similar distances of 3.4−3.7 Å were observed between the reactive atoms for isoprenyl pyrophosphate synthases such as farnesyl pyrophosphate synthase and undecaprenyl pyrophosphate synthase.[39,40] A distance of 4.2 Å is found between C-1 of geranyl diphosphate and a non-natural aromatic substrate in NphB.[34] However, this enzyme might bind substrates in different conformations as indicated by multiple possible locations of prenylation and relaxed specificity for the aromatic substrate. The significance of this distance is unclear. In the case of protein prenyltransferases such as protein farnesyltransferase and protein geranylgeranyltransferase type-I, larger distances of over 7 Å between the peptide substrate and the isoprenoid substrate were reported.[41−43] It was proposed that the prenyl substrate reorients in these enzymes to allow for the prenylation to occur.[43,44] In our crystal structure, all atoms of the indole ring are located further than 4.3 Å away from the C-1 atom of DMSPP. These distances are longer than those observed previously, making regular prenylation difficult. We find, however, that the atoms C-2 and C-3 of the indole nucleus are within 3.8 and 3.5 Å of the C-3 atom of DMSPP, respectively. These distances indicate that a reverse prenylation at one of these positions would be possible. However, the final product of FtmPT1, tryprostatin B, carries a regular prenylation at its C-2 atom, effectively ruling out reverse prenylation as an option for the reaction mechanism. Inspection of the structure alone therefore does not offer a direct pathway to understanding how FtmPT1 achieves its regioselectivity. Nevertheless, the structural data are consistent and in fact support a model in which the prenyl group changes its position during catalysis, allowing regular prenylation (see Discussion).

Redirecting the Regioselectivity of FtmPT1. The main differences in the binding sites of FtmPT1 and FgaPT2 are substitutions of FtmPT1 residue G115 with a threonine, and of FtmPT1 residue H279 with an arginine (Figure 3). Given its location at the rear of the binding pocket, we hypothesized that the residue at position 115 is a key determinant of the regioselectivity of FtmPT1. To test this hypothesis, we performed site-directed mutagenesis experiments with G115.

Mutation of G115 to T reduced formation of tryprostatin B by FtmPT1 to 0.4% of the wild-type activity (Figure 4A).

(39) Hosfield, D. J.; Zhang, Y.; Dougan, D. R.; Broun, A.; Tari, L. W.; Swanson, R. V.; Finn, J. *J. Biol. Chem.* **2004**, *279*, 8526.
(40) Guo, R. T.; Ko, T. P.; Chen, A. P.; Kuo, C. J.; Wang, A. H.; Liang, P. H. *J. Biol. Chem.* **2005**, *280*, 20762.
(41) Strickland, C. L.; Windsor, W. T.; Syto, R.; Wang, L.; Bond, R.; Wu, Z.; Schwartz, J.; Le, H. V.; Beese, L. S.; Weber, P. C. *Biochemistry* **1998**, *37*, 16601.
(42) Long, S. B.; Casey, P. J.; Beese, L. S. *Structure* **2000**, *8*, 209.
(43) Taylor, J. S.; Reid, T. S.; Terry, K. L.; Casey, P. J.; Beese, L. S. *EMBO J.* **2003**, *22*, 5963.
(44) Long, S. B.; Casey, P. J.; Beese, L. S. *Nature* **2002**, *419*, 645.

However, consumption of brevianamide F still occurred at about 17% of the wild-type activity. Mass spectrometry and ^{1}H and ^{13}C NMR analyses including $^{1}H-^{1}H$ correlated spectroscopy (COSY), $^{1}H-^{13}C$ heteronuclear single quantum coherence (HSQC), and $^{1}H-^{13}C$ heteronuclear multiple-bond correlation (HMBC) (Supporting Information, Table S1 and Figures S5−S7) revealed that the G115T mutant catalyzes the formation of a different product that carries a reverse prenyl moiety at the C-3 of the indole nucleus (Figure 4B). In the structure of the identified product, an additional bond between the adjacent nitrogen of the diketopiperazine moiety and the C-2 of the indole nucleus is formed, leading to a pentacyclic system. The most likely interpretation of these data is that the amide performs a nucleophilic attack on the C-2 after reverse prenylation at C-3.[45] Proton abstraction would then have to occur, putatively performed by E102. Nuclear Overhauser effect spectroscopy (NOESY) was used to determine the stereochemistry at C-2 and C-3 (Supporting Information, Figure S8). The new chiral centers at C-3 and C-2 exhibit *R*- and *S*-configurations, respectively (Figure 4B). Products carrying the same prenylation pattern and stereochemistry were previously obtained with the recombinant prenyltransferase CdpC3PT on several cyclic dipeptides.[46] Moreover, products carrying the same prenylation position but with inverted configurations at the indole C-2 and C-3 were observed when using the indole PT AnaPT.[45] As the prenylation has to occur from the opposite side in the case of the AnaPT reaction, we expect that substrate binding occurs in a somewhat different manner in this PT.

We then investigated the effect of other amino acids at position 115 on enzymatic reactivity. Mutation of glycine to alanine (G115A) did not change the prenylation position of FtmPT1, indicating that this small shift can be accommodated by the enzyme. However, mutation to isoleucine (G115I), while still yielding soluble FtmPT1, completely abolished formation of any product. The bulky isoleucine residue in this position probably induces a substantial shift of the aromatic substrate in the binding pocket. Thus, we assume that the essential hydrogen bond to E102 cannot be formed. Interestingly, a G115L variant of FtmPT1 also exhibits formation of a new product, while formation of tryprostatin B is abolished. However, the rate of formation of the new product is only 1% of that of the catalytic rate of wild-type FtmPT1, and the structure of the new product could therefore not be determined in this study. In summary, we have established G115 as an essential regulator of regioselectivity. Furthermore, we were able to re-engineer FtmPT1 to selectively catalyze a reverse prenylation at C-3 of the indole nucleus instead of the regular prenylation at C-2.

Implications for Other Fungal Indole Prenyltransferases. A number of other PTs, including CdpNPT, FgaPT1, FtmPT2, MaPT, 7-DMATS, TdiB, and CpaD, exhibit high sequence similarity to FtmPT1. Although crystal structures for any of these enzymes are not available, sequence comparisons with FtmPT1 nevertheless provide insight into the determinants of the diverse substrate specificities and regioselectivities exhibited by these enzymes (Supporting Information, Figure S9).

It is evident from the sequence alignment that several residues located in the binding sites for both substrates are conserved in all enzymes of this group, an observation that was recently also made by Liu and Walsh.[47] On the basis of the structure−function relationships established here and for the FgaPT2 structure, we can assign specific functions to conserved amino acids. Residue E102 is conserved throughout all sequences, with the exception of TdiB. In TdiB, it is replaced by an aspartic acid residue, which most likely can serve a similar function. In FtmPT1 and FgaPT2, the glutamate is clearly essential as its mutation abolished catalytic activity in both cases. Given its high degree of conservation, participation of this residue in the catalytic cycle of all fungal indole PTs known to date is highly probable.

The pyrophosphate binding site, which is lined with basic residues, is also well conserved. R113 and K294 are present in all aligned sequences. Q380 is replaced with a lysine residue in some PTs, which would also be able to interact with pyrophosphate. K441 is replaced with nonbasic residues in some PTs, but only if the loss of that charge is compensated by substitution of Q380 for lysine. Therefore, we conclude that all fungal indole PTs bind DMAPP very similarly, using multiple positive charges to compensate for the negative charges of the phosphate moieties.

Furthermore, the four tyrosine residues that build up the rigid tyrosine shield are fully conserved in all PTs. This conservation further underscores their essential significance in substrate binding, in reducing the energy barrier to the formation of the carbocation, and in shielding the nascent carbocation from other nucleophiles. The exceptional conservation of the tyrosine shield also further supports a similar structure and binding mode of DMAPP for all fungal indole PTs.

The substrate specificity of fungal indole PTs is likely determined by a small number of residues. The general architecture of the binding pocket can be assumed to be similar in all these enzymes, given the hydrophobic nature of the indole substrate. However, subtle modifications account for changes in size and binding characteristics of this pocket. G115 is essential in determining the substrate specificity and regioselectivity of FtmPT1, as it allows the substrate brevianamide F to penetrate deeply into the binding pocket. In the sequences of FgaPT2 and MaPT, two enzymes catalyzing a regular prenylation at C-4 of the indole nucleus of L-Trp, this glycine residue is replaced with threonine. Furthermore, in both cases, FtmPT1 residue H279 is replaced with an arginine, which in the case of FgaPT2 contacts the carboxylate group of L-Trp.[32] These two modifications substantially decrease the size of the binding site, accounting both for the specificity for L-Trp and its derivatives and the regioselectivity for prenylation at C-4 of the indole nucleus. FtmPT2, which catalyzes the prenylation of 12,13-dihydroxyfumitremorgin C at position N-1 of the indole nucleus, also has a glycine residue at the position of G115. The steric demand of 12,13-dihydroxyfumitremorgin C is somewhat larger than that of brevianamide F due to the methoxy group attached to the indole nucleus. However, it was shown that FtmPT1 was also able to use derivatives of L-Trp that carry methyl groups at positions 4−7 as substrates, indicating that an additional methoxy group can be accommodated if a glycine residue is at the position of G115.[30] In line with these observations, FtmPT1 residue L187 is replaced with threonine in FtmPT2, enlarging the binding pocket further and suggesting a similar binding mode of methoxy-derivatized compounds for FtmPT2. In conclusion, a very small number of amino acids at

(45) Yin, W.-B.; Xie, X.-L.; Matuschek, M.; Li, S.-M. *Org. Biomol. Chem.* **2010**, *8*, 1133.
(46) Yin, W.-B.; Yu, X.; Xie, X.-L.; Li, S.-M. *Org. Biomol. Chem.* **2010**, *8*, 2430.
(47) Liu, X.; Walsh, C. T. *Biochemistry* **2009**, *48*, 11032.

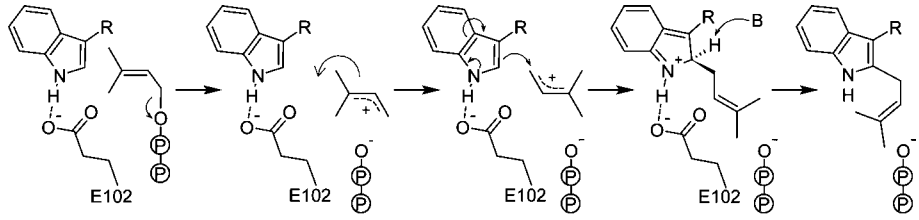

Figure 5. Proposed reaction mechanism of FtmPT1. The aromatic substrate is brevianamide F.

select positions, especially the position of G115 of FtmPT1, are critical determinants of the regioselectivity of fungal indole PTs.

Discussion

We have determined crystal structures of the fungal indole PT FtmPT1 in both its native and substrate-bound states at high resolution. FtmPT1 exhibits a rare PT-barrel fold that to date has only been observed in three other soluble aromatic PTs: FgaPT2, NphB, and CloQ.[32,34,35] Sequence analyses and functional data indicate that key residues important for catalysis and ligand binding are conserved among all fungal indole PTs. We therefore predict that these enzymes all share the same PT-barrel fold as well as the binding mode of DMAPP and essential aspects of the catalytic mechanism. Our analysis also provides additional support for a common evolutionary origin of the bacterial ABBA-PTs and the fungal indole PTs.[32]

In combination with functional data, the crystallographic analysis serves as a solid platform for understanding the reaction mechanism of FtmPT1. Although the positioning of the substrates does not seem to account for the observed regioselectivity of FtmPT1, we believe that both substrates are bound in a way that represents the substrate-bound state of FtmPT1 in solution. The DMAPP binding site is conserved among fungal indole PTs, and the position of the pyrophosphate group is well-defined by the electron density. This binding also limits the freedom of the dimethylallyl group. The second substrate, brevianamide F, is anchored in place by several specific hydrogen bonds. Furthermore, it cannot slide deeper into the binding pocket to bring its atom C-2 closer to the C-1 atom of DMSPP as this would result in steric clashes. Yet, the final product carries a regular prenylation at this C-2 atom. While we cannot rule out conformational changes during the reaction, our data suggest that FtmPT1 does not achieve regioselectivity just by direct positioning of the substrates.

To investigate the apparent discrepancy of substrate binding and regioselectivity, we investigated possible prenylations at the atoms C-2 and C-3 of the indole nucleus in more detail. Prenylation at the atom C-3 of the indole ring, the atom closest to DMSPP, would yield a product unable to undergo rearomatization due to the lack of a hydrogen atom at that position. Thus, we predict that the resulting product would be thermodynamically less stable than the product of prenylation at the atom C-2, which could undergo rearomatization. The C-2 atom lies within 3.8 Å of DMSPP. Although a reverse prenylation at this atom would seem to be possible based on the observed distances in the crystal structure alone, the bulky quaternary carbon would clash with the side chain of Y435. Furthermore, such a reaction is unlikely to occur as the product tryprostatin B features a regular prenylation (Figure 1A).

We considered three possibilities by which FtmPT1 could achieve a direct regular prenylation at C-2. First, a large conformational rearrangement in the protein could take place to reposition the substrates. The structure of FtmPT1 probably does not allow for such a rearrangement, given that the β-barrel is a rigid structure that is stabilized by numerous main-chain hydrogen bonds and exhibits low thermal factors. Second, a chemical rearrangement of the dimethylallylic cation could take place, such as the migration of a methyl group from the atom C-3 to the atom C-2 of DMAPP. This option could be further investigated by isotopic labeling studies. However, we are not aware of any chemical precedence for the shift of a methyl group from a carbocation to an unactivated carbon atom. Third, the planar allylic cation could rotate in the active site. This rotation could occur on a much smaller time scale than the rate-limiting steps of catalysis, and we did not find any counter-arguments for this option. In fact, the relatively weak electron density observed for the dimethylallyl group in our crystal structure (Figure 2C) indicates that this group possesses some mobility. Thus, we propose that the energetically favored product carrying a regular prenylation at the atom C-2 is formed selectively after rotation of the dimethylallylic cation in the active site (Figure 5).

A three-step mechanism was proposed for the DMATS reaction,[38] disregarding the steps of substrate binding and product release (Figure 1B). This mechanism probably represents the basic mechanism of all fungal indole PTs. Hydrolysis of the mixed phosphoryl ester of DMAPP defines the first step. The generated carbocation is attacked by the indole nucleus at position C-1 (regular prenylation) or at C-3 (reverse prenylation) to generate the σ-complex in the second step. Proton abstraction then restores aromaticity and yields the final product in step three. Kinetic isotope effect experiments demonstrated that both ester hydrolysis and carbon−carbon bond formation are partially rate-limiting, while deprotonation is not.[38] In the case of FtmPT1, a rotation of the free carbocation has to occur between the two partially rate-limiting steps. The turnover number k_{cat} of FtmPT1 is 5.57 s^{-1}.[28] Thus, both of the two partially rate-limiting steps occur on time scales that are orders of magnitude larger than that of rotation. Therefore, rotation does not contradict the proposed four-step catalytic cycle (Figure 5).

The catalytic cycle of FtmPT1 requires a base to abstract a proton from the σ-complex. Our mutagenesis studies indicate that E102 does not only serve as a hydrogen-bonding partner, but could also act as a base in the catalytic cycle. Furthermore, the observed cyclization using the amide nitrogen of brevianamide F indicates that this nitrogen atom is capable of performing a nucleophilic attack. Thus, it is also conceivable that it acts as a base in the catalytic cycle. Our mutagenesis data also demonstrate that H279, the only other nearby residue capable of acting as a base, is not involved in catalysis. The most likely scenario is therefore that a proton is abstracted by E102 and possibly relayed by the diketopiperazine moiety.

Our structure−function analysis of FtmPT1 provides insight into several key features of this enzyme and its relatives. It is clear that all fungal indole PTs bind DMAPP, a substrate that

is common to all of them, in a similar manner. The activity of FtmPT1 does not depend on the presence of divalent cations,[28] an observation that was also made for other members of the fungal indole PTs, such as DMATS from *C. purpurea*, FgaPT2, CdpNPT, FgaPT1, and DMATS from *A. fumigatus*.[17] In contrast, absolute requirement for divalent cations such as Mg^{2+} and Mn^{2+} has been reported for several other PTs.[3] While pyrophosphate binding is mediated by divalent cations coordinated by aspartic acid residues in the Mg^{2+}-dependent PTs, fungal indole PTs such as FgaPT2 and FtmPT1 utilize positive charges from the protein environment to neutralize the negatively charged phosphates. Residues that contact the pyrophosphate group are highly conserved in all fungal indole PTs, demonstrating that these enzymes all use the same, metal-ion independent strategy for pyrophosphate binding. Several hydrogen bonds additionally stabilize the DMAPP in the binding sites of FtmPT1 and FgaPT2, and we expect a high degree of conservation for these interactions in other fungal indole PTs as well.

In contrast, the aromatic substrates vary among the fungal indole PTs. The key feature of these enzymes is not a high velocity, as most members of the group exhibit turnover numbers of $0.1-5\ s^{-1}$.[17] Rather, their central hallmark is the conveyance of strict regioselectivity to an otherwise only moderately selective reaction. This is perhaps best demonstrated by the structural comparison of the active sites of FtmPT1 with FgaPT2. Although these two enzymes have generally conserved active site architectures, they modulate the position and orientation of their aromatic substrates efficiently using only a small number of amino acids. FgaPT2 prenylates the C-4 atom within the indole ring system of L-Trp. The larger active site of FtmPT1 is formed as a result of two key substitutions, at positions 115 and 279, which serve to reposition the indole ring system of brevianamide F such that prenylation is unlikely at the positions N-1 and C-4−7. Additional mechanisms then come to play to direct the prenylation toward the atom C-2. Given this knowledge, it should be possible to redirect the regioselectivity of the indole PTs via subtle mutations. We present evidence for such a switch for FtmPT1, which we have been able to modify such that it no longer prenylates the C-2 atom of brevianamide F, but instead targets the C-3 atom. On the basis of this finding, we expect that it is possible to specifically re-engineer different fungal indole PTs, thereby facilitating the process of generating chemoenzymatic libraries. These libraries, in turn, could serve as a basis for high-throughput screening experiments for pharmacologically active compounds.

In summary, fungal indole PTs have great potential for chemoenzymatic synthesis. This group of enzymes exhibits a remarkable flexibility for their aromatic substrates, which is coupled to a rigid scaffold provided by their PT-barrel fold. These enzymes accept tryptophan derivatives with modifications on the side chain and on the indole ring (FgaPT2 and 7-DMATS) or tryptophan-containing cyclic dipeptides (FtmPT1, CdpNPT, AnaPT, and CdpC3PT) as aromatic substrates and prenylate them at different positions of the indole ring.[12] Usually, several prenylated derivatives can be obtained from one substrate by using different prenyltransferases. In most cases, one prenylated derivative is the dominant product. The prenyl transfer reactions catalyzed by these enzymes are not only regiospecific, but also stereospecific.[12] For example, four aszonalenin stereoisomers were produced using AnaPT and CdpNPT as catalysts.[48] Furthermore, AnaPT and CdpC3PT catalyzed the prenylation of cyclic dipeptides at position C-3 of the indole ring with different stereochemistry, resulting in the formation of α- and β-prenylated indolines, respectively.[45,46] These enzymes are soluble proteins and can be produced conveniently in *E. coli* as His-tagged fusion proteins in good yields. Because of these features, they represent excellent prototypes of modifiable bioreactors, especially for production of C-prenylated derivatives, which are usually difficult to prepare chemically. An improved understanding of their underlying catalytic mechanisms may allow for specific modification or even the design of enzymes for the biosynthesis of artificial natural products. In all likelihood, the new products will further expand the fascinating diversity of applications exhibited by these compounds and continue to arouse a significant amount of interest.

Materials and Methods

Protein Expression, Purification, and Crystallization. His-tagged FtmPT1 was purified as described by Grundmann et al.[28] The protein was concentrated to 5 mL using an Amicon Centriprep YM-10 concentrator (Millipore), passed through a 0.2 μm filter, and applied to a Superdex 200 HiLoad 26/60 gel filtration column (GE Healthcare). The column was eluted with 25 mM Tris-HCl pH 8.0, 100 mM NaCl, 2 mM DTT. Fractions containing pure FtmPT1 were pooled, diluted 1:2 with 25 mM Tris-HCl pH 8.0, 2 mM DTT, and concentrated to 5.6 mg mL^{-1} prior to crystallization. Crystals were grown by hanging drop vapor diffusion at 20 °C. On a coverslip, 1 μL of the protein solution was mixed with 1 μL of precipitant solution (1.3 M $(NH_4)_2SO_4$, 0.2 M Li_2SO_4, 0.1 M MES pH 6.5). The coverslip was then sealed with grease over a reservoir containing 500 μL of pure precipitant solution. Crystals grew within 2 days at room temperature and were flash-frozen in liquid nitrogen without the use of a cryoprotectant.

To create the ternary complex containing both substrates, an FtmPT1 crystal was stepwise transferred from its growth condition into a new solution containing 1.3 M Li_2SO_4 and 0.1 M MES pH 6.5 at 20 °C. The crystal was then stepwise transferred into a solution containing 1.3 M Li_2SO_4, 0.1 M MES pH 6.5, 2.5 mM brevianamide F, and 10 mM dimethylallyl *S*-thiolodiphosphate (DMSPP), incubated in that solution for 30 min, and flash-frozen in liquid nitrogen.

Data Collection and Structure Determination. The FtmPT1 crystals belong to space group $P4_12_12$ ($a = b = 82.85$ Å, $c = 121.76$ Å) and contain one monomer in the asymmetric unit. Data for the unliganded FtmPT1 crystals were collected at the Swiss Light Source beamline X06DA in Villigen, Switzerland, using a mar225 CCD detector after annealing the crystal for 5 s.[49] Data for the ternary complex resulted from data collection at the Swiss Light Source beamline X06SA in Villigen, Switzerland, using a Pilatus 6M pixel detector. All diffraction data were recorded at 100 K. Data were reduced using XDS and XSCALE.[50] The same reflections were marked for the free set of reflections in both cases. In addition, 5% of the reflections in the resolution bin of 2.50−2.40 Å were included in the free set for the data of the ternary complex. Data statistics are summarized in Table S2.

The crystal structure of unliganded FtmPT1 was determined at 2.50 Å resolution by molecular replacement with the crystal structure of FgaPT2 (PDB 3I4Z) in PHASER,[51] which yielded a single solution. Ten cycles of simulated annealing were performed in PHENIX[52] to remove the model bias. The output model was

(48) Yin, W.-B.; Cheng, J.; Li, S.-M. *Org. Biomol. Chem.* **2009**, *7*, 2202.
(49) Stevenson, C. E. M.; Mayer, S. M.; Delarbre, L.; Lawson, D. M. *J. Cryst. Growth* **2001**, *232*, 629.
(50) Kabsch, W. J. *J. Appl. Crystallogr.* **1993**, *26*, 795.
(51) McCoy, A. J.; Grosse-Kunstleve, R. W.; Adams, P. D.; Winn, M. D.; Storoni, L. C.; Read, R. J. *J. Appl. Crystallogr.* **2007**, *40*, 658.

then completed through several cycles of manual building in COOT,[53] followed by refinement with REFMAC.[54] The final refinement step involved TLS parametrization[55] using one TLS group per protomer.

The structure of the ternary complex was then determined to a resolution of 2.40 Å by molecular replacement with the unliganded structure using rigid body refinement in REFMAC.[54] Initial difference electron density maps clearly revealed the presence of both substrates in the complex structure. To remove existing model bias, 10 cycles of simulated annealing were carried out in PHENIX.[52] The model was first adjusted to account for any changes in the protein environment by several cycles of manual building in COOT,[53] followed by refinement with REFMAC.[54] Coordinates for both substrates were obtained from the PRODRG server[56] and manually fit into the model to account for the electron density. The final refinement step involved TLS parametrization[55] using one TLS group per protomer. Crystallographic refinement of both structures yielded models that possess low free *R*-factors, excellent stereochemistry, and small root-mean-square deviations from ideal values for bond lengths and bond angles. Refinement statistics are summarized in Table S3. The geometries of the final models were analyzed with PROCHECK[57] and SFCHECK.[58] Figures were generated using MOLSCRIPT.[59]

The atomic coordinates for FtmPT1 and FtmPT1 in complex with both substrates have been deposited with the Protein Data Bank (http://www.rcsb.org) with PDB codes 3O24 and 3O2K, respectively.

Mutagenesis. Mutations were introduced into the *ftmPT1* sequence according to a protocol described previously.[60] The proteins were expressed and purified as described above, and the enzymatic activity was determined as described previously.[28]

Structure Elucidation of the New Product of the G115T Mutant. The new product of the G115T mutant was isolated by HPLC from a 10 mL enzyme assay as described previously[28] and subjected to MS and NMR analyses. Positive electrospray ionization (ESI) mass spectrometry was carried out using an AutoSpec instrument (Micromass Co. UK Ltd.). MS data were as follows: *m*/*z* (intensity) 374 (50) $[M+Na]^+$, 352 (100) $[M+H]^+$. For NMR experiments, 1 mg of the isolated new product of the G115T mutant was dissolved in 0.2 mL of $CDCl_3$ and filled into Wilmad 3 mm tubes (Rototec Spintec). Spectra were recorded at 298 K on a Bruker Avance 600 MHz spectrometer equipped with an inverse probe with *z*-gradient. The HSQC and HMBC spectra were recorded with standard methods.[61] NOESY experiments[62] were performed in phase-sensitive mode using the State-TPPI technique.[63] For all two-dimensional spectra, 32−64 transients were used. For NOESY spectra, a mixing time of 300 ms and a relaxation delay of 3.0 s were applied. ^1H spectra were acquired with 65 536 data points, while 2D spectra were collected using 4096 points in the F_2 dimension and 512 increments in the F_1 dimension. Chemical shifts were referenced to $CDCl_3$. All spectra were processed with Bruker TOPSPIN 2.1.

Acknowledgment. We thank the Swiss Light Source for beam time and are grateful to their staff for support. This work was funded by grants from the Deutsche Forschungsgemeinschaft to S.M.L. (Li844/1-3) and T.S. (SFB766).

Supporting Information Available: Information about the dimer interface, crystallographic refinement, sequence alignments, characterization of the new product, and comparison of the native and substrate-bound states. This material is available free of charge via the Internet at http://pubs.acs.org.

JA106817C

(52) Adams, P. D.; Grosse-Kunstleve, R. W.; Hung, L.-W.; Ioerger, T. R.; McCoy, A. J.; Moriarty, N. W.; Read, R. J.; Sacchettini, J. C.; Sauter, N. K.; Terwilliger, T. C. *Acta Crystallogr., Sect. D: Biol. Crystallogr.* **2002**, *58*, 1948.
(53) Emsley, P.; Cowtan, K. *Acta Crystallogr., Sect. D: Biol. Crystallogr.* **2004**, *60*, 2126.
(54) Murshudov, G. N.; Vagin, A. A.; Dodson, E. J. *Acta Crystallogr., Sect. D: Biol. Crystallogr.* **1997**, *53*, 240.
(55) Winn, M. D.; Murshudov, G. N.; Papiz, M. Z. *Methods Enzymol.* **2003**, *374*, 300.
(56) Schuettelkopf, A. W.; van Aalten, D. M. F. *Acta Crystallogr., Sect. D: Biol. Crystallogr.* **2004**, *60*, 1355.
(57) Laskowski, R. A.; MacArthur, M. W.; Moss, D. S.; Thornton, J. M. *J. Appl. Crystallogr.* **1993**, *26*, 283.
(58) Vaguine, A. A.; Richelle, J.; Wodak, S. J. *Acta Crystallogr., Sect. D: Biol. Crystallogr.* **1999**, *55*, 944.
(59) Fenn, T. D.; Ringe, D.; Petsko, G. A. *J. Appl. Crystallogr.* **2003**, *36*, 944.
(60) Zheng, L.; Baumann, U.; Reymond, J. L. *Nucleic Acids Res.* **2004**, *32*, e115.
(61) Berger, S.; Braun, S. *200 and More NMR Experiments. A Practical Course*; Wiley-VCH: Weinheim, Germany, 2004.
(62) Hwang, T. L.; Shaka, A. J. *J. Am. Chem. Soc.* **1992**, *114*, 3157.
(63) Marion, D.; Ikura, M.; Tschudin, R.; Bax, A. *J. Magn. Reson.* **1989**, *85*, 393.